Published in IET Power Electronics
Received on 8th December 2011
Revised on 18th June 2012
doi: 10.1049/iet-pel.2012.0105

ISSN 1755-4535

Methodology for the optimal design of transformerless grid-connected PV inverters

E. Koutroulis[1] *F. Blaabjerg*[2]

[1]*Department of Electronic & Computer Engineering, Technical University of Crete, Chania GR-73100, Greece*
[2]*Department of Energy Technology, Aalborg University, Aalborg DK-9220, Denmark*
E-mail: efkout@electronics.tuc.gr

Abstract: The transformerless photovoltaic (PV) inverters are the major functional units of modern grid-connected PV energy production systems. In this study, a new optimisation technique is presented for the calculation of the optimal types and values of the components comprising a transformerless PV inverter, such that the PV inverter levelised cost of the generated electricity is minimised. The proposed method constitutes a systematic design process, which is capable to explore the impact of the PV inverter configuration on the trade-off between the PV inverter manufacturing cost and the power losses affecting the corresponding energy production. The design optimisation results demonstrate that the optimal values of the PV inverter design variables depend on the inverter specifications, the technical and economical characteristics of the components used to build the PV inverter and the meteorological conditions prevailing at the installation area. Compared with non-optimised transformerless inverters, the PV inverter structures derived using the proposed design optimisation methodology exhibit lower manufacturing cost and simultaneously are capable of producing more energy into the electric grid system.

1 Introduction

The DC/AC inverters (PV inverters) are the key elements in grid-connected PV energy production systems, since they interface the energy produced by the PV array into the electric grid [1]. Compared with the grid-connected PV inverters with galvanic isolation, the transformerless PV inverters (e.g. full-bridge, NPC and HERIC) have the advantages of lower cost, higher efficiency, smaller size and lower weight [1–3]. A general block diagram of a grid-connected PV system employing a transformerless PV inverter with a full-bridge power section is illustrated in Fig. 1. The power switches of the PV inverter are controlled by a control unit and an output filter is used to reduce the high-order harmonics, thus injecting a sinusoidal current into the electric grid.

The LCL-type output filters are usually used instead of the L- or LC-type filters, since they are capable to achieve attenuation of the switching harmonics using smaller reactive elements and also obtain better decoupling between the filter and the grid impedance [4]. The control unit developed is usually using digital signal processor (DSP) and field programmable gate array (FPGA) ICs [5] for the execution of control and energy management algorithms (e.g. maximum power point tracking (MPPT) [6], modulation strategies [7] etc.), thus constituting a major subsystem of the PV inverter structure, affecting both the energy injected into the electric grid and the PV inverter cost. The optimal design of controller parameters, LC output filter components and the power sharing coefficients for enhancing the stability of an inverter-based micro-grid is presented in [8]. A technique for the design optimisation of a one-cycle controller used in a single-stage inverter, by means of a multi-objective optimisation strategy, is proposed in [9].

As analysed in [10], the stochastically varying solar irradiation and ambient temperature conditions prevailing at the PV array installation site and the shape of the PV inverter efficiency against output power curves define the actual energy injected into the electric grid. An 'ideal' PV inverter would be capable to maximise the energy injected into the electric grid with the minimum possible manufacturing cost. Typically, iterative trial-and-error techniques are employed in the design process of PV inverters, targeting to maximise performance metrics such as the power conversion efficiency at nominal operating conditions or the 'European Efficiency' [1, 11–13]. An optimal LCL-filter design procedure is proposed in [14] for the minimisation of a pulse width modulation (PWM) voltage–source converter output-filter cost and volume. The design process of the LCL-type output filter in a grid-interactive voltage–source inverter is explored in [15]. The total power loss of that filter is used as the optimisation criterion for the selection of optimal values of the filter components. However, these methods have the disadvantage that the impact of the PV inverter component values and operational characteristics (e.g. maximum switching frequency) on both the PV inverter manufacturing cost and the total energy production is not considered during the design process.

In this paper, a new technique for the optimal design of the power section and output filter of transformerless PV inverters is presented. Using the proposed method, the

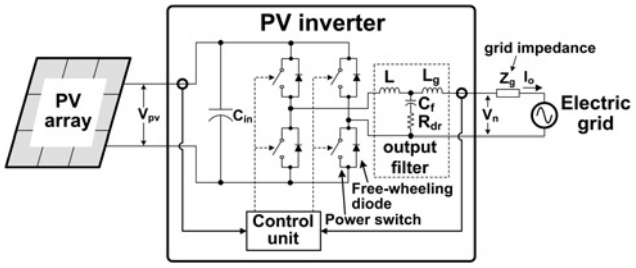

Fig. 1 *Grid-connected PV system employing a transformerless single-phase PV inverter with a full-bridge power section*

optimal types and values of the PV inverter components are calculated such that the PV inverter levelised cost of the generated electricity (LCOE) is minimised, whereas simultaneously considering the limitations imposed by the electric-grid-interconnection regulations and international standards. Compared with the past-proposed approaches applied to design of PV inverters, the method presented in this paper has the advantage that the influences of the PV installation site solar irradiation potential, the PV array operational characteristics and the PV inverter component cost and operational characteristics, on both the PV inverter manufacturing cost and total energy production, are simultaneously taken into account during the PV inverter design process. Thus, the proposed design tool is capable of exploring the impact of the PV inverter configuration (e.g. switching frequency applied, on-state voltage of the power switches etc.) on the trade-off between the PV inverter manufacturing cost and the power losses affecting the corresponding energy production. It comprises a systematic design process targeting to assist the PV inverter designer to derive the optimal PV inverter configuration, without significantly depending on the level of experience from the circuit designed.

The proposed design optimisation methodology is outlined in Section 2, the mathematical model considered during the optimisation procedure is analysed in Section 3 and a design optimisation example is presented in Section 4. Finally, conclusions are drawn.

2 Proposed design optimisation methodology

The target of the proposed design optimisation methodology is to calculate the optimal values of the following PV inverter design variables:

- switching frequency, f_s;
- type of power semiconductors; and
- values of output-filter inductances, L and L_g, capacitance, C_f and damping resistance, R_{dr}.

The optimisation algorithm inputs are the following:

- operational characteristics and configuration (i.e. power rating, open-circuit voltage, number connected in series/parallel etc.) of the PV modules comprising the PV array connected to the PV inverter;
- 1 h average solar irradiance and ambient temperature time-series during the year,
- PV inverter specifications (i.e. nominal output voltage/frequency and power rating) provided by the PV inverter designer;
- PV inverter topology and modulation strategy;
- price and technical characteristics of the power semiconductors comprising the PV inverter power section;
- price and technical characteristics of the magnetic components, capacitors and resistors of the output filter; and
- specifications imposed by electric-grid-interconnection regulations (e.g. the maximum permitted harmonic-current level etc.).

The technical characteristics of the components used to construct the PV inverter are available in the device datasheet provided by the manufacturer, whereas their prices are specified by the market conditions. As in the past-proposed PV inverter design techniques, they are both considered as deterministic parameters in the proposed methodology. The solar irradiation and ambient temperature input data for each geographical location (e.g. based on yearly measurements, the typical meteorological year etc.) are widely available in databases of weather monitoring institutions, since they are also used to design and evaluate the performance of photovoltaic systems [16]. The operational characteristics and configuration of the PV modules and PV inverters comprising the grid-connected PV system are selected by the PV system designer using the techniques described in [17] for the maximisation of the total revenues obtained during the lifetime operation (e.g. 25 years) of the PV installation. Similarly to these methods, the proposed design process of the PV inverter is performed without taking into account the probabilistic uncertainty associated with the meteorological input data [17].

The optimal values of the design variables are calculated such that the PV inverter LCOE (in €/kWh) [18] is minimised, whereas simultaneously the constraints imposed by the PV inverter specifications and electric-grid-interconnection regulations are met

$$\underset{X}{\text{minimise}}\{\text{LCOE}\} = \underset{X}{\text{minimise}}\left\{\frac{C_t}{E_t}\right\} \quad \text{subject to: design specifications and constraints are met} \tag{1}$$

where C_t (€) is the PV inverter total manufacturing cost, E_t (kWh) is the PV inverter total output energy, which is injected into the electric grid during the year and $\boldsymbol{X}$ is the vector of the design variables listed above.

For grid-connected PV installations it is desirable to maximise the net economic benefit obtained by selling the PV-generated energy. This is achieved by minimising the cost per unit energy injected into the electric grid for each individual subsystem of the PV installation (i.e. PV modules, inverters, balance of system components etc.). Thus, the use of LCOE, which involves both design and operational parameters, as an objective function in the proposed method enables to explore, during the design optimisation process, the impact of the PV inverter configuration (e.g. switching frequency applied, on-state voltage of the power switches etc.) on the trade-off between the PV inverter manufacturing cost and the power losses affecting the corresponding energy production. The yearly energy injected by the PV inverter into the electric grid has been included in (1), since it has been considered that, similarly to the process used to design PV systems [17], the same yearly time-series of solar irradiation and ambient

doi: 10.1049/iet-pel.2012.0105

temperature conditions prevail during each year of the PV plant lifetime period.

In the proposed optimisation process, hourly values of the meteorological input data are used to investigate the PV inverter operation during a time period of 1 year, for each set of the design variables values produced by the optimisation algorithm. The management of the relatively high volume of meteorological input data required is easily achieved by developing the proposed optimisation method in the form of a computer program as discussed later in this paper.

A flow-chart of the proposed optimisation procedure is illustrated in Fig. 2. Given the PV inverter specifications and the electric and magnetic characteristics of the components, the violation of the PV inverter operational constraints is explored for each set of design variable values using the appropriate mathematical model of the PV inverter topology, which is under consideration. Then, the objective function of the design optimisation process is evaluated. If any of the constraints is not satisfied or the global optimum of the objective function has not been derived, then a new set of the design variable values is produced by the optimisation algorithm. This procedure is implemented using genetic algorithms (GAs), which are capable to derive the global optimum solution of complex non-linear objective functions with computational efficiency [19].

The basic information unit of a GA-based optimisation process is the chromosome, which corresponds to vector $\boldsymbol{X}$ in (1) and represents a potential solution of the optimisation problem. A population of chromosomes is iteratively modified, thus producing the successive generations of the GA evolution process [19]. At each generation, the objective function is evaluated for all chromosomes of the corresponding population. The chromosome providing the lowest value of the objective function is comprised of the optimal design-parameter values of the PV inverter. This process is repeated until a predefined number of population generations have evolved.

After all combinations of component types input by the PV inverter designer have been optimally designed, the combination with the lowest LCOE and the corresponding design variables values are output as the overall optimal design of the PV inverter. The values of C_t and E_t in (1) are calculated during the optimisation procedure using the PV inverter model are described in the next section.

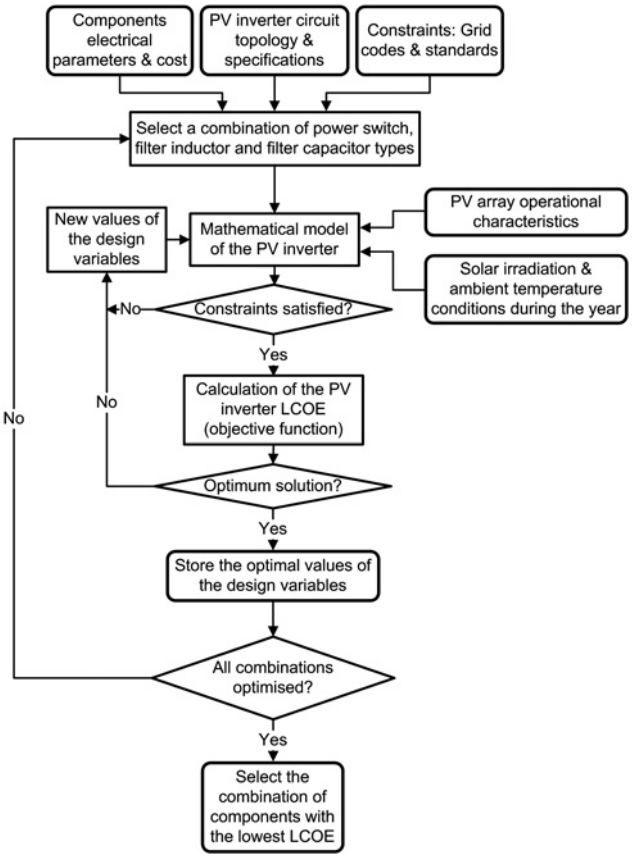

Fig. 2 *Flow-chart of the proposed optimisation procedure for grid-connected single-phase transformerless PV inverters*

3 PV inverter modelling for optimisation

The PV inverter input and output power levels are assumed constant during each 1 h time-step that the PV inverter operation is investigated during the year, as analysed in Section 2. The power switches are controlled using the sinusoidal pulse-width-modulation (SPWM) principle [20]. The PV inverter output filter is considered to have the generalised LCL-type structure illustrated in Fig. 1, consisting of the components L, L_g, C_f and R_{dr}. In case that the PV inverter designer specifies that the PV inverter comprises an L- or LC-type filter, then the values of $[L_g, C_f, R_{dr}]$ or $[L_g, R_{dr}]$, respectively, are set equal to zero during the optimisation process.

The ripple factor, RF_{sw} (%), which is due to the converter-side inductance only, L, is constrained to be less than the maximum permissible limit, $RF_{sw,m}$ (%) [21]

$$RF_{sw} = \frac{I_r(t)V_n}{P_n} \leq RF_{sw,m} \tag{2}$$

where $I_r(t)$ (A) is the root mean square (RMS) value of the switching ripple because of converter-side inductance, L, at hour t ($1 \leq t \leq 8760$), V_n (V) is the PV inverter nominal output voltage (V), and P_n (W) is the PV inverter nominal output power level.

The value of $RF_{sw,m}$ is input to the proposed optimisation process by the PV inverter designer and it is typically selected in the range of 10–25% [21, 22]. The value of RF_{sw} affects the value and size of the converter-side inductance, L. The $L_g - C_f$ part of the LCL-filter will further reduce the current ripple at the PV inverter output, as analysed next.

In case of a full-bridge SPWM inverter (Fig. 1) producing a unipolar output voltage waveform and operating with one fast-switching leg and a slow-switching leg (i.e. 50 Hz), the value of I_r is calculated as follows [23]

$$I_r = \frac{V_{pv}(t)\sqrt{2m_a^2[(\pi/4)(1 + (3m_a^2/4)) - 4(m_a/3)]/3\pi}}{2Lf_s} \tag{3}$$

where $V_{pv}(t, y)$ (V) is the PV array output voltage under MPPT conditions at hour t ($1 \leq t \leq 8760$), m_a is the modulation index and f_s (Hz) is the switching frequency of the fast-switching leg.

The value of m_a is given by

$$m_a = \frac{\sqrt{2\{V_n^2 + [I_o(t)2\pi f(L + L_g)]^2\}}}{V_{PV}(t)} \quad (4)$$

where $I_o(t)$ (A) is the RMS PV inverter output current at hour t ($1 \leq t \leq 8760$), calculated as analysed below and f (Hz) is the PV inverter nominal output frequency.

Depending on the type of the PV inverter output filter specified by the PV inverter designer:

- L- or LC-type output filter: the value of $RF_{sw,m}$ in (2) is equal to the maximum permissible limit, RF_{max} (%);
- LCL-type output filter: the $L_g - C_f$ part of the filter is designed such that the current ripple, which is because of the converter-side inductance only, RF_{sw} in (2), is further reduced below RF_{max} (%) at the PV inverter output

$$RF = RF_{sw} R_a \leq RF_{max} \quad (5)$$

where RF (%) is the ripple factor at the PV inverter output, R_a (%) is the ripple attenuation factor of the LCL filter evaluated at the switching frequency and RF_{max} (%) is the maximum permissible limit of harmonic current distortion at the PV inverter output.

The value of R_a (%) is calculated according to [21] as follows

$$R_a = \frac{i_g(h_s)}{i(h_s)} = \frac{K_d}{|1 + (L_g/L)(1 - LC_b\omega_s^2(C_f/C_b))|} \quad (6)$$

where h_s is the order of the switching frequency harmonic, $i_g(h_s)$ and $i(h_s)$ are the grid- and converter-side currents, respectively, at the switching frequency, K_d is a factor accounting for the reduction in filter effectiveness because of damping, C_b is the base capacitance [$C_b = P_n/(V_n^2 2\pi f)$] and $\omega_s = 2\pi f_s$. Additionally, in order to ensure that resonance problems in the lower and upper parts of the harmonic spectrum are avoided, the LCL-filter resonant frequency, f_{res} (Hz), is selected as follows

$$10f \leq f_{res} \leq \frac{f_s}{2} \quad (7)$$

where $f_{res} = (1/2\pi)\sqrt{(L + L_g)/L_g C_f L}$.

The value of RF_{max} is selected such that the current ripple at the PV inverter output is reduced at an acceptable level, in order to comply with the limits imposed by grid regulations and international standards (e.g. IEEE-519 and IEEE-1547) [14].

The total value of the PV inverter output filter inductance is restricted to be less than 0.1 pu in order to limit the AC voltage drop during operation, thus enhancing the dynamic response of the PV inverter [4, 21]

$$L + L_g \leq 0.1L_b \quad (8)$$

where L_b is the base inductance $L_b = V_n^2/(P_n 2\pi f)$.

In order to limit the power loss because of reactive current circulation, the value of the LC- or LCL-filter capacitor, C_f, is selected such that its reactive power is less than 5% of the rated power

$$C_f \leq 0.05C_b \quad (9)$$

In the case of an LCL-type output filter, the damping resistor value, R_{dr} (Ω), is set equal to the filter capacitor impedance at the resonant frequency, otherwise it is set equal to zero

$$R_{dr} = \begin{cases} \dfrac{1}{C_f 2\pi f_{res}} & \text{for LCL-type filter} \\ 0 & \text{for } L\text{-or LC-type filters} \end{cases} \quad (10)$$

The design process of the PV inverter is performed assuming that the electric grid operates under nominal frequency (i.e. 50 Hz) conditions [21, 23]. Since the SPWM principle is applied in order to control the power switches, the PV inverter switching frequency, f_s, is constrained to be an integer multiple of the nominal grid frequency, f (Hz). Additionally, the maximum possible value of f_s is dictated by the maximum switching-speed capability of the power switches, $f_{s,max}$ (Hz), specified by their manufacturer

$$f_s \leq f_{s,max} \quad (11)$$

It is assumed that an efficient MPPT is performed by the PV inverter control unit, such that the maximum available PV power is supplied to the PV inverter [6]. The total energy injected into the electric grid by the PV inverter during the year, E_t (Wh), is calculated from a power-balance equation as follows

$$E_t = \sum_{t=1}^{8760} P_o(t)\,\Delta t = \sum_{t=1}^{8760} [P_{PV}(t) - P_l(t)]\,\Delta t \quad (12)$$

where $P_o(t)$, $P_{PV}(t)$ and $P_l(t)$ (W) is the power injected into the grid by the PV inverter, the PV array output power under MPPT conditions and the PV inverter total power loss, respectively, at hour t ($1 \leq t \leq 8760$) and Δt is the simulation time-step ($\Delta t = 1$ h).

The PV inverter total power loss, P_l (W), is equal to the sum of the power losses of the individual components and subsystems comprising the PV inverter

$$P_l(t) = P_{cond} + P_{sw} + P_d + P_{L,c} + P_{L,r} + P_{cu} \quad (13)$$

where P_{cond} and P_{sw} (W) are the power section switches and diodes total conduction and switching losses, respectively, P_d (W) is the power loss on the LCL-filter damping resistor, $P_{L,c}$ and $P_{L,r}$ (W) are the LCL-filter inductors total core and winding losses, respectively, and P_{cu} (W) is the power consumption of the control unit (because of the circuits of the SPWM modulator, power switch drivers, sensors and signal conditioners etc.) and cooling system.

In (13), the power semiconductor conduction and switching losses, P_{cond} and P_{sw}, respectively, are calculated as the sum of the conduction and switching losses of the individual power switches and diodes forming the power section of the PV inverter. For the calculation of the power semiconductor conduction losses, P_{cond}, the PV inverter power switches and diodes are considered as voltage

doi: 10.1049/iet-pel.2012.0105

sources with resistors connected in series [24]

$$V_s = V_{s,on} + I_s R_{s,on} \tag{14}$$

$$V_d = V_{d,f} + I_d R_{d,f} \tag{15}$$

where V_s and V_d (V) are the voltage drops across the power switch and diode, respectively, I_s and I_d (A) are the conduction current of the power switch and diode, $V_{s,on}$ (V), $R_{s,on}$ (Ω) are the power switch on-state voltage and resistance and $V_{d,f}$ (V), $R_{d,f}$ (Ω) are the diode forward voltage and resistance.

The average power loss during conduction of each power switch and diode of the PV inverter, P_s and P_d (W), is then calculated based on (14) and (15), according to the following equations

$$P_s = V_{s,on} I_{s,avg} + I_{s,rms}^2 R_{s,on} \tag{16}$$

$$P_d = V_{d,f} I_{d,avg} + I_{d,rms}^2 R_{d,f} \tag{17}$$

where $I_{s,avg}$, $I_{d,avg}$ (A) are the average values of the power switch and diode current, respectively, and $I_{s,rms}$, $I_{d,rms}$ (A) are the RMS values of the power switch and diode current, respectively.

The values of $I_{s,avg}$, $I_{d,avg}$, $I_{s,rms}$ and $I_{d,rms}$ in (16) and (17) depend on the PV inverter power section topology (e.g. full-bridge and H5) under consideration. The switching losses in (13), P_{sw}, are equal to the sum of the power switches turn-on and turn-off losses as well as the reverse recovery losses of the power diodes. They are calculated to be proportional to the switching frequency, f_s, the turn-on and turn-off energy, E_{on} (J) and E_{off} (J), respectively, and the peak load current of the PV inverter, as analysed in [24]. The values of $V_{s,on}$, $R_{s,on}$, $V_{d,f}$, $R_{d,f}$, E_{on} and E_{off} are specified by the power semiconductor manufacturer and they are input to the proposed optimisation process by the PV inverter designer.

The power loss on the LCL-filter damping resistor, P_d (W), depends on the RMS current of the damping resistor, $I_{dr,rms}$ (A)

$$P_d(t) = I_{dr,rms}^2 R_{dr} = \left[\frac{V_n^2 + [I_o(t) 2\pi f L_g]^2}{(1/2\pi f C_f)^2 + R_{dr}^2} + I_r^2(t) \right] R_{dr} \tag{18}$$

where R_{dr} (Ω) is the damping resistor value.

The total core losses of the LCL-filter inductors, $P_{L,c}$ (W), are calculated according to [25], whereas simultaneously considering that the optimisation process guarantees the satisfaction of (5), which permits to neglect the high-frequency current ripple flowing through the filter inductor L_g [21]

$$P_{L,c}(t) = k_f m_a^{-a} (f_s/1000)^{-b} p_{c-1} L \left[I_o(t) \sqrt{2L} \right]^c + p_{c-1} L_g \left[I_o(t) \sqrt{2L_g} \right]^c \tag{19}$$

where k_f is a constant expressing the impact of the non-sinusoidal excitation, PWM modulation index, switching frequency and inductor volume, respectively, on the inductor core loss, a, b and c are constants dependent on the inductor core material and p_{c-1} is the inductor core-loss factor under sinusoidal excitation ($W/[H(\sqrt{HA})^c]$).

The total power loss on the windings of the LCL-filter inductors, $P_{L,r}$ (W), is calculated according to the RMS current of each inductor, as follows:

$$P_{L,r}(t) = I_r^2(t) r_l L + I_o^2(t) r_l (L + L_g) \tag{20}$$

where r_l (Ω/H) is the winding resistance of the inductances normalised per unit inductance.

The values of c, p_{c-1} and r_l in (18)–(20) are specified by the inductor manufacturer. The parameters k_f, a and b are estimated according to the procedure described in [25] and their values, together with those of c, p_{c-1} and r_l, are input in the proposed optimisation process by the PV inverter designer.

The power loss models presented above have been considered in the proposed methodology because of their simplicity. Since the optimisation process is modular, the proposed methodology can also be applied for the design optimisation of any PV inverter topology (e.g. NPC and Active-NPC) if the appropriate power-loss models (e.g. those presented in [2, 26]) are used to calculate the conduction and switching losses of the power semiconductors employed in that topology.

The PV inverter output current, $I_o(t)$ (A), is calculated using a numerical analysis method from the power-balance equation

$$P_{pv}(t) = P_l(t) + V_n I_o(t) \tag{21}$$

The values of V_{pv} and P_{pv} in (3), (4), (12) and (21) are calculated on an hourly basis during the year using the PV modules model analysed in [27], based on the solar irradiation and ambient temperature time-series, the electrical specifications of the PV modules and their configuration (i.e. connection in series and parallel) within the PV array, which are input in the proposed optimisation procedure by the PV inverter designer.

The total manufacturing cost of the PV inverter, C_t (€), is equal to the sum of the prices of the components comprising the PV inverter

$$C_t = c_{inv} P_n + n_s c_s + n_d c_d + c_i (L + L_g) \frac{P_n}{V_n} + c_c C_f + \mathrm{SF}\, c_r R_{dr} P_{d,max} \tag{22}$$

where c_{inv} (€/W) is the PV inverter manufacturing cost, comprising the costs of labour and raw materials, without including the cost of the power switches, diodes and output filter components (e.g. control unit, heat-sinks and printed circuit boards etc.), n_s and n_d are the number of power switches and diodes, respectively, comprising the PV inverter power section, c_s, c_d (€) are the cost of each power switch and diode, respectively, c_i [€/(HA)] is the filter inductors cost per unit inductance and current rating, c_c (€/F) is the filter capacitor cost per unit capacitance, c_r [€/(Ω·W)] is the filter damping resistor cost per unit resistance and power, SF (%) is the damping resistor over-sizing factor and $P_{d,max}$ (W) is the maximum power dissipated on the damping resistor during the year.

The value of $P_{d,max}$ is calculated based on the damping resistor power loss during the year given by (18), as follows

$$P_{d,max} = \max_{1 \le t \le 8760} \{P_d(t)\} \tag{23}$$

In the proposed methodology, the PV inverter design process described in Section 2 is performed by calculating the values of E_t and C_t in (1) using (12) and (22) and simultaneously it is subject to the constraints defined by inequalities (2), (5), (7)–(9) and (11).

4 Design optimisation example

The proposed methodology has been applied for the optimal design of a transformerless single-phase/full-bridge PV inverter interconnected with the electric grid (Fig. 1) with $P_n = 2000$ W, $V_n = 220$ V and $f = 50$ Hz. The power switches are controlled according to the unipolar SPWM modulation strategy with one fast-switching leg and a slow-switching leg. The PV inverter under study is connected to a PV array composed of 12 PV-modules connected in series (total area = 15 m^2). The maximum power point (MPP) power and voltage ratings of each PV module, under standard test conditions (STC), are 175 W and 35.4 V, respectively.

The decision variables considered during the design optimisation procedure are the PV inverter power semiconductors type, the switching frequency and the values of the LCL-filter components. Thus, in the proposed optimisation methodology each GA chromosome corresponds to vector $\boldsymbol{X}$ in (1) and consists of four genes (i.e. L, L_g, C_f and f_s) in the form: $\boldsymbol{X} = [L|L_g|C_f|f_s]$. After the GA-based optimisation process described in Section 2 has been accomplished, the optimal value of the LCL-filter damping resistor, R_{dr}, is calculated according to (10) using the resulting optimal values of L, L_g and C_f. The values of P_{cond} and P_{sw} in (13) have been calculated using the equations of the power-loss model presented in [24] as a function of L, L_g, f_s, V_n, f, $I_o(t)$, $V_{PV}(t)$ and the conduction and switching operational characteristics of the power switches and free-wheeling diodes under consideration, specified by their manufacturer. The maximum permissible output current ripple has been set to $RF_{max} = 4\%$ in order to comply with the IEEE-1547 standard, whereas the maximum limit of the ripple factor because of the converter-side inductance only has been set to $RF_{sw,m} = 20\%$ according to [21, 22].

Two different types of IGBT-type power switches with free-wheeling diodes are considered as potential alternatives for incorporation in the PV inverter power section. As analysed in Section 2, the proposed optimisation process is separately performed for each of these two types in order to derive the overall optimum configuration. In this design optimisation example, it is assumed that the power semiconductors are mounted on heat sinks with convection cooling, thus the cooling system does not consume any power. The technical characteristics of commercially available power switches and free-wheeling diodes considered in this design optimisation example are presented in Table 1. In the technical characteristics of the LCL output filter inductors shown in Table 2, the values of k_f a, b, c and p_{c-l} have been extracted from [15, 28], whereas that of r_l is based on the corresponding values of commercially available power inductors. The filter effectiveness due to damping is reduced by $K_d = 1.57$ [21] and the damping resistor over-sizing factor has been empirically set equal to SF = 110%. Similarly to commercially available PV inverters of the same power rating, the control unit power consumption has been set equal to $P_{cu} = 5$ W. The economical characteristics of the PV inverter components considered in the optimisation process are based on the selling prices of the corresponding components in the international market and they are tabulated in Table 3. Considering the cost of PV inverters in [29, 30] as well as after conducting a survey of the international market, the value of c_{inv} in (22) has been set equal to 355 €/kW.

A software program operating under the MATLAB platform has been developed in order to implement the proposed design tool. The GA functions available in the library of the MATLAB Global Optimisation Toolbox have been used to develop the GA-based evolution program in order to derive the global minimum of the PV inverter LCOE function. The GA process has been executed for $G = 200$ generations with $N = 70$ chromosomes in each generation.

The optimal values of the PV inverter LCL output filter components (L, L_g, C_f and R_{dr}), switching frequency, f_s and LCOE, calculated using the proposed optimisation technique for the two alternative types of power switches in the case of PV inverters installed at various sites in Europe, are summarised in Table 4. A different set of optimal values of the PV inverter design variables is derived in each case, since each installation site is characterised by different solar irradiation and ambient temperature conditions.

The two types of power switches achieve equivalent performance in terms of PV inverter LCOE in Murcia (Spain). In the rest of the installation sites considered, the minimum LCOE is obtained using the power switch type 1, because although of lower switching-speed capability compared with power switch type 2, it exhibits lower on-state voltage and cost, which better match the PV array energy production at these sites. In all cases examined, the optimal switching frequency of PV inverters built using power switch type 1 has been calculated to be near to the maximum permissible value imposed by the power switch

Table 2 Technical characteristics of the LCL output filter inductors of the PV inverter

k_f	α	b	c	p_{c-l}	r_l, Ω/H
5.42	1.21	0.09	0.058	1747	8

Table 3 Economical characteristics of the PV inverter components

c_{inv}, €/kW	$c_s + c_d$, €	c_i, €/(HA)	c_c, €/F	c_r, €/(ΩW)
355	type 1:1.5 type 2:3	832	134×10^3	3.6×10^{-3}

Table 1 Technical characteristics of the PV inverter power switches and free-wheeling diodes

	$V_{s,on}$, V	$R_{s,on}$, mΩ	$V_{d,f}$, V	$R_{d,f}$, mΩ	E_{on}, mJ	E_{off}, mJ	$F_{s,max}$, kHz
type 1	0.75	83.3	0.87	120	0.09	0.11	30
type 2	1.05	37.1	1.1	47	0.58	0.25	80

doi: 10.1049/iet-pel.2012.0105

Table 4 Optimal values of the PV inverter design variables and LCOE for various installation sites in Europe

	Power switch	L, mH	L_g, μH	C_f, μF	R_{dr}, Ω	f_s, kHz	LCOE, €/kWh
Athens (Greece)	type 1	1.459	48.121	5.608	2.882	28.85	0.223
	type 2	1.361	39.508	5.661	2.604	31.45	0.225
Murcia (Spain)	type 1	1.682	59.610	5.906	3.122	25.10	0.198
	type 2	0.873	19.189	5.154	1.909	47.65	0.198
Freiburg (Germany)	type 1	1.463	43.651	5.921	2.676	29.50	0.323
	type 2	1.519	48.172	5.209	2.994	29.45	0.327
Oslo (Norway)	type 1	1.557	38.272	6.577	2.383	29.55	0.328
	type 2	1.475	38.644	6.063	2.492	30.80	0.331

operational capabilities, thus aiming towards the reduction of the output filter size and cost. The optimal design results presented in Table 4 indicate that the LCL-filter is the optimal output filter type for the installation sites considered, since in the case that an L- or LC-type filter was more appropriate, then the optimal values of L_g and/or C_f derived by applying the proposed optimisation process would be calculated to approach zero. The optimal LCOEs for each installation site deviate by less than 1.24%, whereas the corresponding deviations between the optimal values of the design variables are in the range of 0.17–89.4%. Since the objective function is characterised by such a low sensitivity close to each optimal solution, in case that under practical operating conditions the design parameters L, L_g, C_f and R_{dr} deviate from the optimal values presented in Table 4, the resulting deviation of the PV inverter LCOE will practically be negligible.

The optimal values of LCOE and total energy injected into the electric grid during the year (i.e. E_t in (1) and (12)) for each installation site of the optimised PV inverter comprising the type 1 power switches, are illustrated in Figs. 3*a* and *b*, respectively. The minimum optimal LCOE is achieved in Murcia (Spain) although, compared to the rest optimised PV inverter structures, the corresponding optimal cost of the PV inverter is higher in this case (Fig. 4). This is due to the high availability of solar irradiation at that area, which results in increased energy to be injected into the electric grid by the optimised PV system. In case that the PV inverter optimised for Murcia (Spain) is installed in either Athens (Greece), Freiburg (Germany) or Oslo (Norway), then the PV inverter output current ripple constraint of the optimisation process, expressed by the inequality in (5), is violated.

The LCOE and yearly energy production of a non-optimised PV inverter comprised of type 1 power switches and operating at $f_s = 8$ kHz, which is a typical switching frequency value in this power range [1, 2], are also depicted in Fig. 3. The non-optimised PV inverter is comprised of an LCL output filter, which has been designed as analysed in [21] with $L = 5.65$ mH, $L_g = 1.09$ mH, $C_f = 3.29$ μF and $R_{dr} = 5.6\ \Omega$. Thus, the non-optimised PV inverter has been designed without considering the manufacturing cost and yearly energy production. Compared with the non-optimised PV inverter, using the proposed design method the optimised PV inverter LCOE is reduced by 9.6–12.7% and the PV-generated energy injected into the electric grid is increased by 4.9–8.6%.

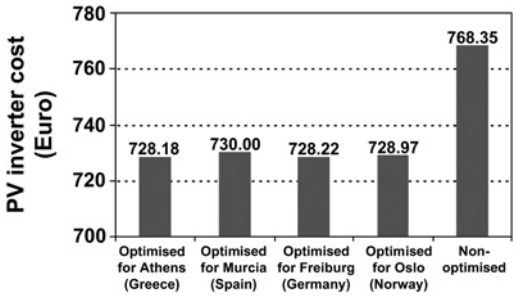

Fig. 4 *Cost of PV inverters optimised for various installation sites and the cost of the non-optimised PV inverter*

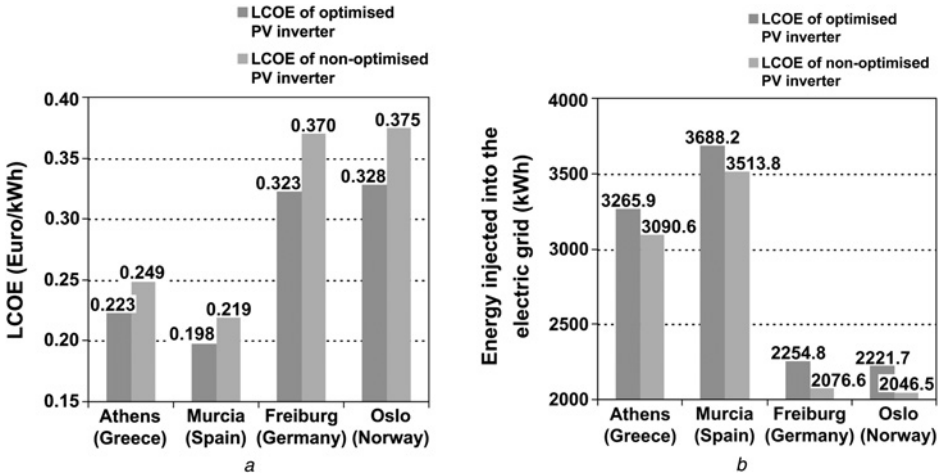

Fig. 3 *Optimised and non-optimised PV inverters for various installation sites in Europe*

a LCOE

b Yearly energy injected into the electric grid for 12 PV modules (total area = 15 m^2)

As illustrated in Fig. 4, the cost of the optimised PV inverters depends on the installation site, whereas, additionally, the non-optimised PV inverter cost is higher by 5.3–5.5%. Depending on the installation site, the efficiency at maximum AC power and the European efficiency of the optimised PV inverters comprising the type 1 power switches vary in the range 96.69–96.73 and 94.71–94.99%, respectively (Fig. 5). The corresponding values of the non-optimised PV inverter are lower by 2.50–2.54 and 6.92–7.20%, respectively. Although the lowest efficiency at maximum AC power and European efficiency values have been obtained for the PV inverter optimised for Murcia (Spain), as demonstrated in Fig. 3 that inverter also exhibits the lowest LCOE value. Efficiencies of the same level have also been reported in [1] for commercially available non-optimised transformerless PV inverters, which, however, have not been designed considering the manufacturing cost/energy production trade-off.

In order to demonstrate an example of the optimisation problem search-space, the plot of the PV inverter LCOE against the decision variables C_f and L_g, in case that a PV inverter comprising type 1 power switches is installed in Murcia (Spain) and $L = 1.682$ mH and $f_s = 25.1$ kHz, is shown in Fig. 6.

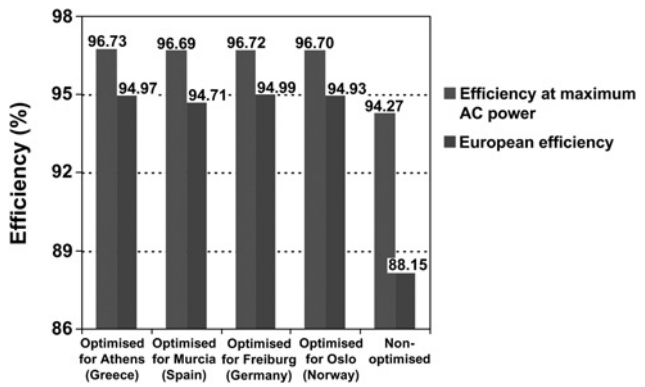

Fig. 5 *Efficiency at maximum AC power and European efficiency of PV inverters optimised for various installation sites in Europe and of the non-optimised PV inverter*

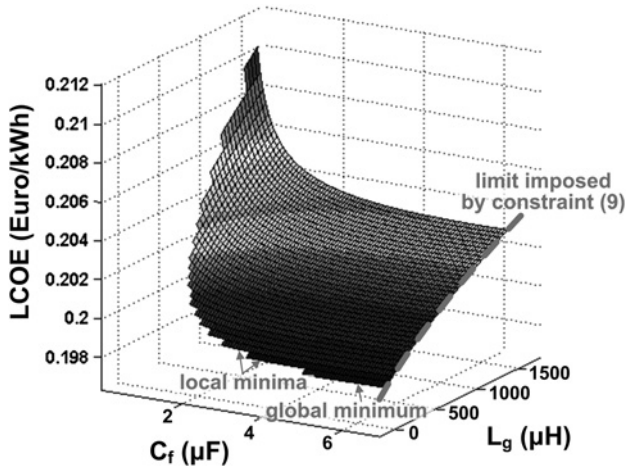

Fig. 6 *PV inverter LCOE against the values of the decision variables C_f and L_g, which satisfy the optimisation problem constraints, in the case that a PV inverter comprising type 1 power switches is installed in Murcia (Spain) and $L = 1.682$ mH and $f_s = 25.1$ kHz*

This diagram has been constructed using only the values of C_f and L_g, which satisfy the optimisation problem constraints. It is observed that the LCOE function is highly non-linear and exhibits multiple local minima, thus dictating the use of a computationally efficient optimisation algorithm, such as GAs, in order to derive the global optimum values of C_f and L_g, which minimise the PV inverter LCOE.

5 Conclusions

The transformerless PV inverters are the major functional units of modern grid-connected PV energy production systems. In this paper, a systematic design process for the optimal design of transformerless PV inverters has been presented. The proposed method embraces optimisation at both the converter-circuit and the circuit-device levels, using information about the solar irradiation potential of the PV installation site and the limitations imposed by the electric-grid-interconnection regulations. The design optimisation results demonstrate that in sharp contrast to the non-optimised PV inverters designed using conventional techniques, where the installation-area-specific meteorological conditions are not considered during the design process, the PV inverter structures derived using the proposed methodology exhibit lower LCOE and manufacturing cost, while simultaneously are capable of injecting more PV-generated energy into the electric grid. Thus, by installing the PV inverters, which have been optimally designed using the proposed design optimisation methodology considering both design and operation parameters, the earnings achieved by the installed PV capacity are increased.

6 References

1 Kerekes, T., Teodorescu, R., Rodríguez, P., Vázquez, G., Aldabas, E.: 'A new high-efficiency single-phase transformerless PV inverter topology', *IEEE Trans. Ind. Electron.*, 2011, **58**, (1), pp. 184–191
2 Xiao, H.F., Xie, S.J., Yang, C., Huang, R.H.: 'An optimized transformerless photovoltaic grid-connected inverter', *IEEE Trans. Ind. Electron.*, 2011, **58**, (5), pp. 1887–1895
3 Blaabjerg, F., Iov, F., Kerekes, T., Teodorescu, R.: 'Trends in power electronics and control of renewable energy systems'. 14th Int. Power Electronics and Motion Control Conf. (EPE/PEMC), 2010, pp. 1–19
4 Cha, H., Vu, T.-K.: 'Comparative analysis of low-pass output filter for single-phase grid-connected photovoltaic inverter'. 2010 25th Annual IEEE Applied Power Electronics Conf. and Exposition (APEC), 2010, pp. 1659–1665
5 Guerrero, J.M., Blaabjerg, F., Zhelev, T., *et al.*: 'Distributed Generation: toward a new energy paradigm', *IEEE Ind. Electron. Mag.*, 2010, **4**, (1), pp. 52–64
6 Pai, F.S., Chao, R.M., Ko, S.H., Lee, T.S.: 'Performance evaluation of parabolic prediction to maximum power point tracking for PV array', *IEEE Trans. Sust. Energy*, 2011, **2**, (1), pp. 60–68
7 Ma, L., Jin, X., Kerekes, T., Liserre, M., Teodorescu, R., Rodriguez, P.: 'The PWM strategies of grid-connected distributed generation active NPC inverters'. Proc. IEEE Energy Conversion Congress and Exposition (ECCE), 2009, pp. 920–927
8 Hassan, M.A., Abido, M.A.: 'Optimal design of microgrids in autonomous and grid-connected modes using particle swarm optimization', *IEEE Trans. Power Electron.*, 2011, **26**, (3), pp. 755–769
9 Fortunato, M., Giustiniani, A., Petrone, G., Spagnuolo, G., Vitelli, M.: 'Maximum power point tracking in a one-cycle-controlled single-stage photovoltaic inverter', *IEEE Trans. Ind. Electron.*, 2008, **55**, (7), pp. 2684–2693
10 Koutroulis, E., Blaabjerg, F.: 'Design optimization of grid-connected PV inverters'. 26th Annual IEEE Applied Power Electronics Conf. and Exposition (APEC), 2011, pp. 691–698
11 Vazquez, G., Kerekes, T., Rolan, A., Aguilar, D., Luna, A., Azevedo, G.: 'Losses and CMV evaluation in transformerless grid-connected PV topologies'. IEEE Int. Symp. Ind. Electron., 2009, pp. 544–548
12 Kjaer, S.B., Blaabjerg, F.: 'Design optimization of a single phase inverter for photovoltaic applications'. 34th Annual IEEE Power Electronics Specialist Conf. (PESC), 2003, vol. 3, pp. 1183–1190

doi: 10.1049/iet-pel.2012.0105

13 Kashihara, Y., Itoh, J.: 'Parameter design of a five-level inverter for PV systems'. IEEE Eighth Int. Conf. on Power Electronics and ECCE Asia (ICPE & ECCE), 2011, pp. 1886–1893
14 Zeng, G., Rasmussen, T.W., Teodorescu, R.: 'A novel optimized LCL-filter designing method for grid connected converter'. Second IEEE Int. Symp. on Power Electronics for Distributed Generation Systems (PEDG), 2010, pp. 802–805
15 Channegowda, P., John, V.: 'Filter optimization for grid interactive voltage source inverters', *IEEE Trans. Ind. Electron.*, 2010, **57**, (12), pp. 4106–4114
16 Lin, C.H., Hsieh, W.L., Chen, C.S., Hsu, C.T., Ku, T.T.: 'Optimization of photovoltaic penetration in distribution systems considering annual duration curve of solar irradiation', *IEEE Trans. Power Syst.*, 2012, **27**, (2), pp. 1090–1097
17 Kornelakis, A., Koutroulis, E.: 'Methodology for the design optimisation and the economic analysis of grid-connected photovoltaic systems', *IET Renew. Power Gener.*, 2009, **3**, (4), pp. 476–492
18 Campbell, M., Blunden, J., Smeloff, E., Aschenbrenner, P.: 'Minimizing utility-scale PV power plant LCOE through the use of high capacity factor configurations'. 34th IEEE Photovoltaic Specialists Conf., 2009, pp. 421–426
19 Michalewicz, Z.: 'Genetic algorithms + data structures = evolution programs' (Springer-Verlag, 1994, 2nd edn.), pp. 15–18
20 Nge, C.L., Midtgard, O.-M., Norum, L., Saetre, T.O.: 'Power loss analysis for single phase grid-connected PV inverters'. 31st Int. Telecommunications Energy Conf., 2009, pp. 1–5
21 Liserre, M., Blaabjerg, F., Hansen, S.: 'Design and control of an LCL-filter-based three-phase active rectifier', *IEEE Trans. Ind. Appl.*, 2005, **41**, (5), pp. 1281–1291
22 Wei, X., Xiao, L., Yao, Z., Gong, C.: 'Design of LCL filter for wind power inverter'. 2010 World Non-Grid-Connected Wind Power and Energy Conf. (WNWEC), 2010, pp. 1–6
23 Kim, H., Kim, K.-H.: 'Filter design for grid connected PV inverters'. IEEE Int. Conf. Sustainable Energy Technologies, 2008, pp. 1070–1075
24 Pattnaik, S.K., Mahapatra, K.K.: 'Power loss estimation for PWM and soft-switching inverter using RDCLI'. Int. MultiConf. Engineers and Computer Scientists, 2010, pp. 1401–1406
25 Tadsuan, S., Tangsiriworakul, C.: 'Design and comparison of iron losses mathematical model with single phase and three phase PWM inverter supply'. IEEE Int. Conf. on Ind. Technol. (ICIT), 2008, pp. 1–6
26 Tehrani, K.A., Rasoanarivo, I., Sargos, F.-M.: 'Power loss calculation in two different multilevel inverter models (2DM2)', *Electr. Power Syst. Res.*, 2011, **81**, (2), pp. 297–307
27 Lorenzo, E.: 'Solar electricity – Engineering of photovoltaic systems' (Progensa, 1994, 1st edn.), pp. 87–99
28 Shimizu, T., Iyasu, S.: 'A practical iron loss calculation for AC filter inductors used in PWM inverters', *IEEE Trans. Ind. Electron.*, 2009, **56**, (7), pp. 2600–2609
29 Chen, S., Peng, L., Brady, D., Lehman, B.: 'Optimum inverter sizing in consideration of irradiance pattern and PV incentives'. 2011 26th Annual IEEE Applied Power Electronics Conf. and Exposition (APEC), 2011, pp. 982–988
30 Xue, Y., Divya, K.C., Griepentrog, G., Liviu, M., Suresh, S., Manjrekar, M.: 'Towards next generation photovoltaic inverters'. 2011 IEEE Energy Conversion Congress and Exposition (ECCE), 2011, pp. 2467–2474